*J. Phys. Chem. A* **2002,** *106,* 8716−8720

# Tuning Spin-State Preference by Substituents: A Case Study of Thianthrene Dication

**Akihiro Ito, Haruhiro Ino, Hidehisa Ichiki, and Kazuyoshi Tanaka***

*Department of Molecular Engineering, Graduate School of Engineering, Kyoto University, Sakyo-ku, Kyoto, 606-8501, Japan*

*Received: November 30, 2001; In Final Form: June 16, 2002*

We report an effective example of $\pi$-conjugated systems showing the reverse spin-state preferences depending on the substitution patterns. It is shown that 2,3,7,8- and 1,4,6,9-tetramethoxy-substituted thianthrenes have different electronic structures owing to destabilization of the specific frontier molecular orbitals. On the basis of the hybrid Hartree−Fock/density functional method (B3LYP/6-31G*), the singlet−triplet energy gaps are estimated to be −10.7 and +8.8 kcal/mol for 2,3,7,8- and 1,4,6,9-substituted thianthrenes, respectively. Moreover, it is also shown that nuclear independent chemical shift (NICS), the index of local aromaticity for polycyclic $\pi$-conjugated systems, is closely correlated with the spin-state preferences of the present thianthrene system.

## I. Introduction

The control of the spin-state preferences of organic polyradicals is not only intriguing per se but also highly desirable in connection with molecule-based magnets.[1] To date, there exists a versatile rule for obtaining high-spin organic molecules for non-Kekulé molecules.[2−6] Many researchers have proposed the rule from different angles, which claims that in short, the connectivity between the spin-containing and magnetic coupling units determines the spin-state preference (the so-called "topology rule"). In particular, the idea of connecting radical centers through 1,3- or 1,3,5-positions of benzene has led to realization of a number of very high-spin organic molecules.[7−9] In this strategy, it is now known both experimentally and theoretically that perturbation effects due to heteroatom substitutions into the molecular skeleton are not crucial for the spin-state preference. However, in the charged system, the expected predictions are no longer effective.[10] Moreover, a large twist angle between the benzene and radical center planes violates the topology rule.[11,12] For the ground-state spin multiplicity of the 10,10′-phenylenediphenothiazine dication, for instance, it was exemplified that the para-linked isomer is triplet whereas the meta-linked one is singlet, contrary to the known topology rule.[13] In this case, the converse spin-state preference is probably derived from the above-mentioned two factors. More seriously, once we look into organic radicals other than non-Kekulé ones, there are no rules for designing high-spin organic molecules.

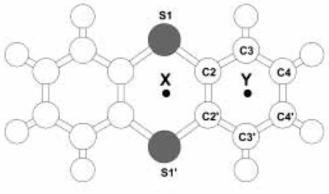

**1**

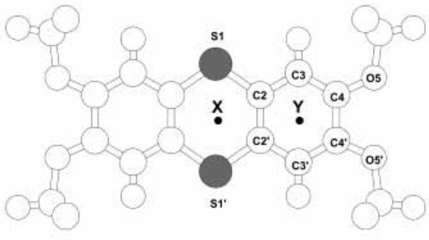

**2**

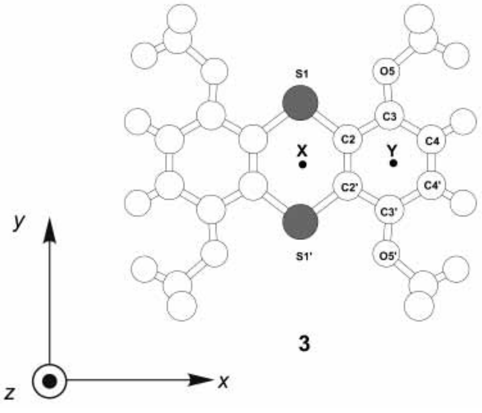

**3**

Here we would like to mention the most typical example in which the spin-state preference is ambiguous. In 1976, Goldberg et al. investigated the spin state for the dication of a derivative of thianthrene (**1**), 2,3,7,8-tetramethoxythianthrene (**2**).[14] The EPR measurements supported the triplet ground state of $\mathbf{2}^{2+}$. Since then, however, reinvestigations about the spin state of $\mathbf{2}^{2+}$ have never been carried out. On the other hand, Bock and co-workers reported interesting results on the X-ray structure of $\mathbf{2}^{2+}$.[15] According to their findings, $\mathbf{2}^{2+}$ in the solid state has a so-called "double-barreled" cyanine structure[16] in which the C−C bonds lengthen along the short molecular axis, and this structural change was ascribed to development of the polymethine moieties due to extension of $\pi$-conjugation onto the substituted methoxy groups. However, strictly speaking, the formed polymethine moieties do not meet the standard cyanine

10.1021/jp0155967 CCC: $22.00

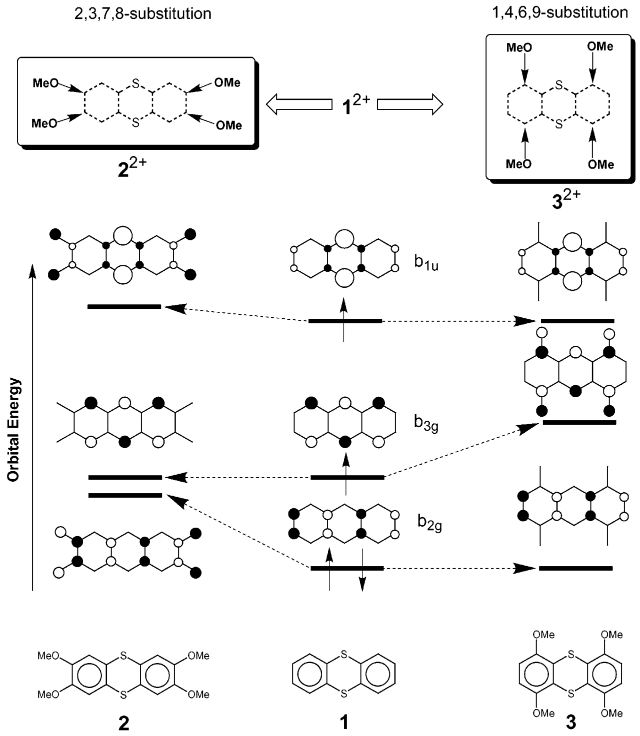

**Figure 1.** Schematic drawing of the frontier MOs of $\mathbf{1}^{2+}$ and the changes in the relative orbital energy levels by orbital interactions with four methoxy groups.

rule.[17] More noteworthy is that in ref 15 they implicitly postulated the closed-shell structure of $\mathbf{2}^{2+}$. Furthermore, it is apparent that the topology rule[11,12] does not account for the actual spin state of $\mathbf{2}^{2+}$.

With such a background, it would be interesting to revisit the relation between the peculiar structure and the spin state of $\mathbf{2}^{2+}$, in conjunction with substitution of methoxy groups. In this article, we have undertaken the detailed description of the electronic structures of $\mathbf{2}^{2+}$ and examined its related thianthrene cation radicals on the basis of quantum chemical calculations.

## II. Outline of Tuning Spin-State Preference of Thianthrene Di(cation radical) by Substituting Methoxy Groups

In this section, we discuss how to tune the spin state of thianthrene di(cation radical) from the viewpoint of orbital interactions. It is helpful to describe the features of the frontier molecular orbitals (MOs) of thianthrene dication ($\mathbf{1}^{2+}$) prior to the elaborate computational analysis. In Figure 1, the qualitative $\pi$-MOs for hypothetical planar $\mathbf{1}^{2+}$ are provided for explanation of the possible orbital interactions due to methoxy substitutions. The frontier MOs of $\mathbf{1}^{2+}$ are depicted in the middle part of the figure and let us pay attention to the orbital coefficients at the 2,3,7,8-positions. Both the upper singly occupied MO (SOMO) ($b_{1u}$) and the doubly occupied MO ($b_{2g}$) have relatively large coefficients at those carbon atoms, whereas the lower SOMO ($b_{3g}$) has almost no coefficients. On the other hand, the lower SOMO ($b_{3g}$) has large coefficients at the 1,4,6,9-positions. Generally speaking, the energy levels of the frontier MOs are raised by substitution of methoxy groups, owing to the out-of-phase orbital interactions. Therefore, when the methoxy groups are substituted into the 2,3,7,8-positions (**2**) or at the 1,4,6,9-positions (**3**), the energy levels are predicted to change drastically. The putative MOs for $\mathbf{2}^{2+}$ and $\mathbf{3}^{2+}$ are shown in both sides in Figure 1. As is evident from these orbital interactions, $\mathbf{3}^{2+}$ has the possibility that the energy difference between two SOMOs becomes fairly smaller than that of $\mathbf{2}^{2+}$. This designates that $\mathbf{3}^{2+}$ has a stronger triplet-state preference than $\mathbf{2}^{2+}$. We next carry out the detailed quantum chemical calculations of $\mathbf{1}^{2+}$, $\mathbf{2}^{2+}$, and, moreover, hypothetical derivative $\mathbf{3}^{2+}$.[18]

**TABLE 1: Bond Lengths (Å) and the NICS Values at Positions X and Y (ppm) for 1, $\mathbf{1}^{+}$, and $\mathbf{1}^{2+}$ at the B3LYP/6-31G* Level**

| | $\mathbf{1}^{a,b}$ $^1A_1(C_{2v})$ | $\mathbf{1}^{+}$ $^2B_{1u}(D_{2h})$ | $\mathbf{1}^{2+}$ $^1A_g(D_{2h})$ | $^3B_{3u}(D_{2h})$ |
|---|---|---|---|---|
| S1···S1′ | 3.258 | 3.469 | 3.424 | 3.483 |
| C2−C2′ | 1.404<br>(1.394(4)) | 1.418 | 1.451 | 1.418 |
| C4−C4′ | 1.396<br>(1.381(5), 1.385(5)) | 1.408 | 1.424 | 1.392 |
| S1−C2 | 1.787<br>(1.769(3), 1.771(3), 1.773(3)) | 1.746 | 1.714 | 1.741 |
| C2−C3 | 1.400<br>(1.387(4), 1.393(4), 1.398(5)) | 1.411 | 1.414 | 1.413 |
| C3−C4 | 1.394<br>(1.370(4), 1.376(5), 1.383(4), 1.384(5)) | 1.383 | 1.381 | 1.406 |
| X | −5.4 | −10.0 | −9.4 | 1.7 |
| Y | −14.3 | −13.7 | −10.9 | −4.3 |

[a] The folding angle $\phi$ is 129.4°. The experimental value at 295 K is 128.09(5)° (see ref 27). [b] The experimental values at 295 K are in parentheses (see ref 27).

## III. Method of Calculations

The geometries described in this study were fully optimized at a hybrid Hartree−Fock/density functional (HF/DF) method (B3LYP) that combines Becke's three-parameter nonlocal exchange functional[19] with the nonlocal correlation functional of Parr and co-workers[20] using the 6-31G* basis set.[21] A single polarization function was added on hydrogens of hydrogenated species. For the species with spin multiplicity, the unrestricted B3LYP (UB3LYP) methods were employed. Magnetic shieldings and nuclear independent chemical shifts (NICS)[22] were also evaluated using the gauge-independent atomic orbital (GIAO) method[22] with the 6-311G* basis set[23] at the B3LYP/6-31G* optimized geometries. All the calculations were performed with the GAUSSIAN 98 package of the ab initio MO programs.[24]

## IV. Results and Discussion

**Thianthrene.** We first start with the examination of the electronic structures of the neutral through dicationic states of the parent compound **1**. In Table 1, the optimized bond lengths of **1**, $\mathbf{1}^{+}$, and $\mathbf{1}^{2+}$ are listed. As for the neutral form, the molecule takes a butterfly conformation, being folded along the axis penetrating two sulfur atoms, as shown in Figure 2. The calculated geometrical parameters including the folding angle $\phi$ (129.4°) are in good agreement with the reported X-ray structure.[25−27] As pointed out by Bock and co-workers,[15] planar **1** is regarded as a 16$\pi$-electron molecular system with excess $\pi$ electrons compared to planar anthracene with "ideal" 14$\pi$ electron structure, owing to substitution of two sulfur atoms. This fact gives a simple account that **1** has a nonplanar conformation. As shown in Figure 3, however, it was confirmed that the potential energy surface is considerably shallow to a large extent due to the folding angle $\phi$, suggesting the ease of the flapping motion.

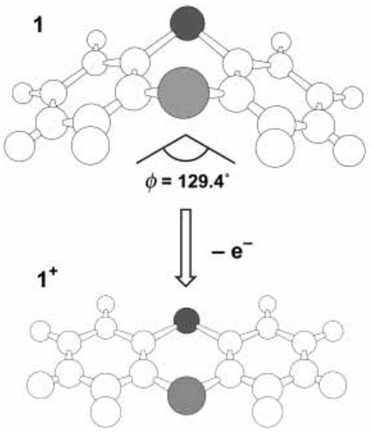

**Figure 2.** Butterfly conformation of **1** and the planarity of $\mathbf{1}^+$.

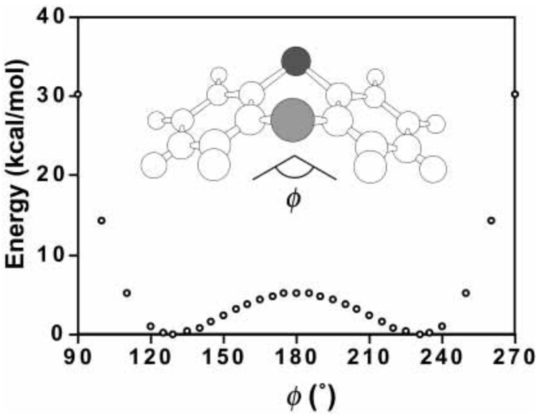

**Figure 3.** Relative energy (kcal/mol) vs folding angle $\phi$ (deg) of thianthrene **1**. At each point, all the geometrical parameters except for the folding angle were optimized by the B3LYP/6-31G* calculations.

Next, although the present calculation predicts a planar conformation of $\mathbf{1}^+$, it has 15$\pi$ electrons, which still does not yet meet the "ideal" 14$\pi$-electron structure. However, taking account of the fact that **1** is subject to deformation near the optimized folding angle, we can conclude that the stabilization energy due to extension of $\pi$-conjugation arising from planar conformation easily exceeds the loss of energy due to deformation from the butterfly conformation. In corroboration of the above phenomena, we calculated the nuclear independent chemical shift (NICS) proposed by Schleyer and co-workers.[22] It was confirmed that aromatic and antiaromatic rings are classified to have negative and positive NICS values, respectively.[22] As shown in Table 1, the NICS for the central dithiin moiety was found to have a negative value (−10.0) comparable to that of the lateral benzene rings (−13.7) in going from **1** to $\mathbf{1}^+$. Moreover, the C−S bond length is shortened by 0.04 Å, whereas the C−C bonds are elongated by 0.014 and 0.012 Å for C2−C2′ and C4−C4′, respectively. This conclusion comes from the fact that an electron is removed from the HOMO ($4b_{1u}$) of **1** (see Figure 4).

On the other hand, there exist two possibilities for the spin multiplicity of $\mathbf{1}^{2+}$, that is, singlet and triplet. The calculated singlet−triplet energy difference, $\Delta E_{S-T}$ was −11.2 kcal/mol, indicating that the ground state is singlet. Here it is noteworthy that Schleyer and co-workers reported that the spin multiplicity of 4n$\pi$-electron annulenes is well correlated with their NICS, that is, their aromaticity.[28] The criterion for the spin multiplicity is offered by the large negative NICS. For instance, according to their calculations, the triplet state of the cyclopentadienyl cation is more stable than the corresponding singlet state where the NICS values were estimated to be −4.5 and +49.2 ppm for the triplet and singlet states, respectively.[28] The calculated NICS on the central dithiin ring is positive for the triplet and negative for the singlet. Moreover, on the lateral benzene rings in the triplet, the NICS shows a small negative value (−4.3 ppm) compared with the value −10.9 for the singlet. Thus the criterion works well for **1**.

The optimized structures for the singlet and triplet states of $\mathbf{1}^{2+}$ reflect the difference of their frontier MO patterns (Figure 4). As for the singlet, the bond lengths of C2−C2′ and C4−C4′ are considerably lengthened by 0.033 and 0.016 Å, as compared with those of $\mathbf{1}^+$. On the contrary, the S1−C2 bond length decreases further by 0.032 Å, obviously because the $4b_{1u}$ orbital becomes vacant. In contrast to such deformation on the molecular skeleton of the singlet $\mathbf{1}^{2+}$, the geometrical features for the triplet $\mathbf{1}^{2+}$ are rather similar to those for $\mathbf{1}^+$ and, consequently, the slight shortening of the lateral C4−C4′ bond occurs, as is evident from (i) the nonbonding character of the $3b_{3g}$ orbital and, in addition, (ii) the in-phase pattern at the lateral bonds of the $4b_{1u}$ orbital.

With these results for the electronic structures of the parent molecule **1**, $\mathbf{1}^+$, and $\mathbf{1}^{2+}$, we can proceed to the analysis of the tetramethoxy-substituted thianthrenes **2** and **3**.

**2,3,6,7-Tetramethoxythianthrene.** As is already described in the Introduction, compound **2** has been examined experimentally in detail by several researchers. Therefore, the molecular structures for **2**, $\mathbf{2}^+$, and $\mathbf{2}^{2+}$ are known by X-ray crystallographic studies.[15,29,30] The optimized bond distances for each structure are provided in Table 2 together with experimental ones. Again, the calculated bond lengths are in good agreement with the experimental results, showing a tendency that the S1−C2 and C4−O5 bond lengths become shortened and the C2−C2′ and C4−C4′ bond lengths lengthened with each oxidation stage. As pointed out by Bock and co-workers, the B3LYP/6-31G* optimizations reproduced the "double-barreled" cyanine structure of $\mathbf{2}^{2+}$ fairly well. The experimental structure is similar to one for the singlet state, although the apparent difference between the optimized structures for the singlet and triplet states are not seen. The similarity between the singlet and triplet structures can be ascribed to destabilization of the $2b_{2g}$ orbital of $\mathbf{1}^{2+}$ due to tetramethoxy substitution.

Generally speaking, out-of-phase orbital interactions take place for the MOs having large coefficients at the carbon centers where the methoxy groups are introduced. These orbital interactions destabilize the $4b_{1u}$ and $2b_{2g}$ orbitals of **1** relative to the $3b_{3g}$, which has negligible coefficients at the 2,3,7,8-positions and results in a crossing of the orbital energy levels between the $3b_{3g}$ and $2b_{2g}$ orbitals of **1**. Therefore, the resulting two SOMOs ($6b_{1u}$ and $4b_{2g}$) of $\mathbf{2}^{2+}$ have bonding character on the C2−C2′ and C4−C4′, leading to the similarity of the structures between the singlet and triplet states. However, because the reported X-ray structure[15] of $\mathbf{2}^{2+}$ is similar to the optimized structure for the singlet $\mathbf{2}^{2+}$ rather than to that for the triplet $\mathbf{2}^{2+}$, it can be predicted that $\mathbf{2}^{2+}$ prefers the singlet state in the crystalline state. In accordance with the geometrical features, the calculated $\Delta E_{S-T}$ for $\mathbf{2}^{2+}$ was estimated to be −10.7 kcal/mol at the B3LYP/6-31G* level, indicating the singlet ground state. The estimated $\Delta E_{S-T}$ values for $\mathbf{1}^{2+}$ and $\mathbf{2}^{2+}$ were essentially the same value, which is probably due to the similar orbital energy difference between two SOMOs for each dication (0.87 eV for $\mathbf{1}^{2+}$; 1.06 eV for $\mathbf{2}^{2+}$). This result is also supported by examining the calculated NICS. The local aromaticity of the lateral benzene rings of the triplet $\mathbf{2}^{2+}$ decreases considerably, as well as that of the central dithiin ring, in contrast with high

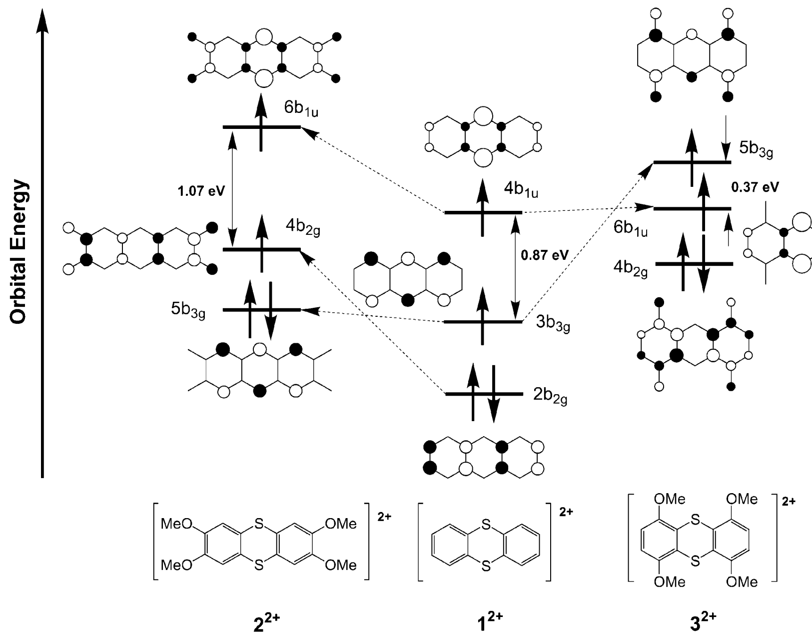

**Figure 4.** Schematic drawings of the frontier MOs for $\mathbf{1}^{2+}$, $\mathbf{2}^{2+}$, and $\mathbf{3}^{2+}$ at the B3LYP/6-31G* level.

**TABLE 2: Bond Lengths (Å) and the NICS Values at Positions X and Y (ppm) for 2, $2^{+}$, and $2^{2+}$ at the B3LYP/6-31G* Level**

| | $\mathbf{2}^{a,b}$ | $\mathbf{2}^{+\,c}$ | $\mathbf{2}^{2+\,d}$ | |
|---|---|---|---|---|
| | $^1A_1(C_{2v})$ | $^2B_{1u}(D_{2h})$ | $^1A_g(D_{2h})$ | $^3B_{3u}(D_{2h})$ |
| S1···S1′ | 3.244 | 3.468 | 3.423 | 3.503 |
| C2−C2′ | 1.393 | 1.410 | 1.439 | 1.432 |
| | (1.383) | (1.395) | (1.453) | |
| C4−C4′ | 1.420 | 1.440 | 1.463 | 1.460 |
| | (1.410) | (1.430) | (1.472) | |
| S1−C2 | 1.788 | 1.752 | 1.729 | 1.761 |
| | (1.776) | (1.723) | (1.695) | |
| C2−C3 | 1.406 | 1.409 | 1.402 | 1.393 |
| | (1.397) | (1.400) | (1.401) | |
| C3−C4 | 1.391 | 1.387 | 1.393 | 1.402 |
| | (1.380) | (1.362) | (1.387) | |
| C4−O5 | 1.361 | 1.336 | 1.310 | 1.310 |
| | (1.369) | (1.349) | (1.315) | |
| X | −5.9 | −9.9 | −14.4 | 0.6 |
| Y | −15.6 | −13.4 | −11.9 | −1.6 |

[a] The folding angle $\phi$ is 128.4°. The experimental value is 131° (see ref 29). [b] The experimental values are in parentheses (see ref 29). [c] The experimental values are in parentheses (see ref 30). [d] The experimental values are in parentheses (see ref 15).

**TABLE 3: Bond Lengths (Å) and the NICS Values at Positions X and Y (ppm) for 3, $3^{+}$, and $3^{2+}$ at the B3LYP/6-31G* Level**

| | $\mathbf{3}^{a}$ | $\mathbf{3}^{+\,b}$ | $\mathbf{3}^{2+}$ | |
|---|---|---|---|---|
| | $^1A_1(C_{2v})$ | $^2B_{3g}(D_{2h})$ | $^1A_g(D_{2h})$ | $^3B_{2u}(D_{2h})$ |
| S1···S1′ | 3.300 | 3.552 | 3.545 | 3.502 |
| C2−C2′ | 1.396 | 1.392 | 1.391 | 1.414 |
| | | (1.425(7)) | | |
| C4−C4′ | 1.400 | 1.378 | 1.361 | 1.383 |
| | | (1.429(7)) | | |
| S1−C2 | 1.785 | 1.775 | 1.767 | 1.739 |
| | | (1.751(5), 1.758(5)) | | |
| C2−C3 | 1.416 | 1.423 | 1.431 | 1.433 |
| | | (1.377(7), 1.378(7)) | | |
| C3−C4 | 1.391 | 1.411 | 1.436 | 1.410 |
| | | (1.414(7), 1.411(7)) | | |
| C4−O5 | 1.367 | 1.340 | 1.313 | 1.325 |
| | | (1.390(6), 1.393(6)) | | |
| X | −5.4 | −1.7 | 0.4 | −1.4 |
| Y | −15.5 | −7.7 | −6.8 | −11.7 |

[a] The folding angle $\phi$ is 133.4°. [b] The experimental values are in parentheses (see ref 31).

local aromaticity for each ring of the singlet $\mathbf{2}^{2+}$. These results are inconsistent with the conclusion from the previous EPR analysis for $\mathbf{2}^{2+}$ in frozen solution.[14]

**1,4,6,9-Tetramethoxythianthrene.** When methoxy groups are substituted at the 2,3,7,8-positions, the $4b_{1u}$ and $2b_{2g}$ orbitals of **1** are perturbed by the out-of-phase orbital interactions. At the B3LYP/6-31G* level, however, the spin preference remains unchanged. These results lead us to consider another substitution pattern, 1,4,6,9-tetramethoxy substitution. In contrast, the $3b_{3g}$ orbital of **1** has solely large coefficients at the 1,4,6,9-positions, and hence, introduction of methoxy groups at these positions destabilizes the (HO−1)MO. This should diminish the difference between the energy levels of two SOMOs ($5b_{3g}$ and $6b_{1u}$), leading to the triplet spin preference of $\mathbf{3}^{2+}$, as shown in Figure 4. As expected, substantial perturbation arises in $\mathbf{3}^{2+}$. The difference between the energy levels of two SOMOs becomes small (0.37 eV), as compared with that of $\mathbf{2}^{2+}$ (1.06 eV). As a result, $\Delta E_{\mathrm{S-T}}$ was calculated to be 8.8 kcal/mol, favoring the triplet ground state of $\mathbf{3}^{2+}$. Influenced by this substitution effect, the SOMOs of $\mathbf{3}^{2+}$ are reversed in comparison with those of $\mathbf{1}^{2+}$, and the optimized structure drastically changes in $\mathbf{3}^{2+}$, as listed in Table 3. Note that the optimized structure for $\mathbf{3}^{+}$ fails to reproduce the X-ray structure for the related compound **4**, where two benzene rings are fused at the 2,3- and 7,8-positions, in its complex with TCNQ.[31] This is probably because the charge transfer in the TCNQ complex of **4** is imperfect. In contrast to $\mathbf{2}^{2+}$, the C2−C2′ and C4−C4′ bond lengths of **3** decreas with increasing oxidation stage, except for those of the

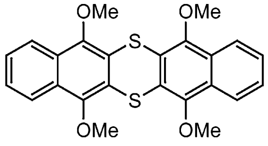

**4**

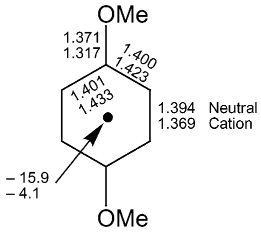

**Figure 5.** Optimized geometry (Å) for 1,4-dimethoxybenzene (**5**) and **5**$^{+}$ at the B3LYP/6-31G* level and their NICS values (ppm) computed at the GIAO-HF/6-311G* level.

triplet **3**$^{2+}$. This shortening of the C−C bonds along the short molecular axis can be explained by electron depletion of the $5b_{3g}$ orbital of **3** having an out-of-phase MO pattern on the C2−C2′ and C4−C4′ bonds. Here it is noteworthy that the structure concerning the lateral benzene moieties of the singlet **3**$^{2+}$ resembles the semiquinone due to the methoxy substitution. Actually, we carried out the B3LYP/6-31G* and the NICS calculations for 1,4-dimethoxybenzene (**5**). Judging from the calculated results shown in Figure 5, the bond lengths of **5**$^{+}$ match well with those of the corresponding moieties for the singlet **3**$^{2+}$(Table 3). Furthermore, both of them take the similar NICS (−4.1 ppm for **5**$^{+}$; −6.8 ppm for **3**$^{2+}$). Therefore we can regard the electronic structure of the singlet **2**$^{3+}$ as that of the two semiquinone bridged by two sulfur atoms. This description is supported by the long S1−C2 bond (1.767 Å). On the other hand, in the triplet **3**$^{2+}$, the C2−C2′ and C4−C4′ bonds are elongated as compared to those of the singlet **3**$^{2+}$. In addition, the S1−C2 bond of **3**$^{2+}$ becomes shorter. More importantly, the NICS values of the central dithiin ring and the lateral benzene ring for the triplet **3**$^{2+}$ are calculated to be −1.4 and −11.7 ppm, indicating a larger local aromaticity than those for the corresponding singlet **3**$^{2+}$. In all, when four methoxy groups are substituted into the 1,4,6,9-positions of the parent molecule **1**, destabilization of the specific frontier orbital is greatly enhanced, and finally, leads to a change in the sign of the singlet−triplet gap.

## V. Conclusion

To assess the substitution effects for spin preferences of non-Kekulé planar $\pi$-systems, we showed that thianthrene molecule **1**, one of the well-known sulfur-containing polycyclic compounds, is an effective model that changes its spin-state preference depending on the substitution patterns. By substituting four methoxy groups into the 2,3,7,8-positions of **1**, the spin state for the ground state of **1**$^{2+}$ remains unchanged at the B3LYP/6-31G* level. This would require reexamination of the spin multiplicity for the ground state of **2**$^{2+}$ determined by EPR spectroscopy to be triplet about 25 years ago. Instead, in 1,4,6,9-tetramethoxy-substituted thianthrene **3**, the specific frontier MO is destabilized, causing a significant stabilization of the triplet state. Therefore there exists the possibility of the triplet ground state of **3**$^{2+}$. This awaits experimental verification. Last, throughout the current work, it was found that the NICS values have a good correlation with the spin preference for $\pi$-conjugated systems.

## References and Notes

(1) Rajca, A *Chem. Rev.* **1994**, *94*, 871.
(2) Mataga, N. *Theor. Chim. Acta* **1968**,*10*, 372.
(3) Borden, W. T.; Davidson, E. R. *J. Am. Chem. Soc*. **1977**,*99*, 4587.
(4) Ovchinnikov, A. A. *Theor. Chim. Acta* **1978**, *47*, 297.
(5) Borden, W. T. *Mol. Cryst. Liq. Cryst*. **1993**, *232*, 195.
(6) Dougherty, D. A. *Acc. Chem. Res*. **1991**, *24*, 88.
(7) Nakamura, N.; Inoue, K.; Iwamura, H.; Fujioka, T.; Sawaki Y. *J. Am. Chem. Soc*. **1992**, *114*, 1484.
(8) Nishide, H.; Miyasaka M.; Tsuchida E. *Angew. Chem., Int. Ed. Engl.* **1998**, *37*, 2400.
(9) Rajca, A.; Rajca, S.; Wongsriratanakul, J. *J. Am. Chem. Soc*. **1999**, *121*, 6308.
(10) West, A. P., Jr.; Silverman, S. K.; Dougherty, D. A. *J. Am. Chem. Soc*. **1996**, *118*, 1452.
(11) Kanno, F.; Inoue, K.; Koga, N.; Iwamura, H. *J. Am. Chem. Soc*. **1993**, *115*, 847.
(12) Fang, S.; Lee, M.-S.; Hrovat, D. A.; Borden, W. T. *J. Am. Chem. Soc*. **1995**, *117*, 6727.
(13) Okada, K.; Imakura, T.; Oda, M.; Murai, H. *J. Am. Chem. Soc*. **1996**, *118*, 3047.
(14) Goldberg, I. B.; Crowe, H. R.; Wilson, G. S.; Glass, R. S. *J. Phys. Chem*. **1976**, *80*, 988.
(15) Bock, H.; Rauschenbach, A.; Ruppert, K.; Havlas, Z. *Angew. Chem., Int. Ed. Engl.* **1991**, *30*, 714.
(16) Wudl, F.; Koutentis, P. A.; Weitz, A.; Ma. B.; Strassner, T.; Houk, K. N.; Khan, S. I. *Pure Appl. Chem*. **1999**, *71*, 295.
(17) Fabian, J.; Hartmann, H. *Light Absorption of Organic Colorants*; Springer: New York, 1980; Chapter 12.
(18) However, the related compounds, 5,7,12,14-tetramethoxydibenzo-[*b,i*]thianthrene[27] and 2,3,7,8-tetramethyl-1,4,6,9-tetramethoxythianthrene were synthesized so far: González, M.; de Miguel, P.; Martín, N.; Segura, J. L.; Seoane, C.; Ortí, E.; Viruela, R.; Viruela, P. M. *Adv. Mater*. **1994**, *6*, 765.
(19) Ragavachari, K. *Theor. Chem. Acc*. **2000**, *103*, 361 and references therein.
(20) Lee, C.; Yang, W.; Parr, R. G. *Phys. Rev. B* **1988**, *37*, 785.
(21) Hehre, W. J.; Radom, P.; Schleyer, P. v. R.; Pople, J. A. *Ab Initio Molecular Orbital Theory*; Wiley: New York, 1986.
(22) Schleyer, P. v. R.; Maerker, A.; Dransfeld, H.; Jiao, H.; van Hommes, N. J. R. *J. Am. Chem. Soc*. **1996**, *118*, 6317.
(23) Wolinski, K.; Hilton, J. F.; Pulay, P. *J. Am. Chem. Soc*. **1990**, *112*, 8251.
(24) Frisch, M. J.; Trucks, G. W.; Schlegel, H. B.; Scuseria, G. E.; Robb, M. A.; Cheeseman, J. R.; Zakrzewski, V. G.; Montgomery, J. A.; Stratmann, R. E., Jr.; Burant, J. C.; Dapprich, S.; Millam, J. M.; Daniels, A. D.; Kudin, K. N.; Strain, M. C.; Farkas, O.; Tomasi, J.; Barone, V.; Cossi, M.; Cammi, R.; Mennucci, B.; Pomelli, C.; Adamo, C.; Clifford, S.; Ochterski, J.; Petersson, G. A.; Ayala, P. Y.; Cui, Q.; Morokuma, K.; Malick, D. K.; Rabuck, A. D.; Raghavachari, K.; Foresman, J. B.; Cioslowski, J.; Ortiz, J. V.; Baboul, A. G.; Stefanov, B. B.; Liu, G.; Liashenko, A.; Piskorz, P.; Komaromi, I.; Gomperts, R.; Martin, R. L.; Fox, D. J.; Keith, T.; Al-Laham, M. A.; Peng, C. Y.; Nanayakkara, A.; Challacombe, M.; Gill, P. M. W.; Johnson, B.; Chen, M.; Wong, W.; Andres, J. L.; Gonzalez, C.; Head-Gordon, M.; Replogle, E. S.; Pople, J. A. *Gaussian 98,* Revision A.9; Gaussian Inc.: Pittsburgh, PA, 1998.
(25) Lynton, H.; Cox, E. G. *J. Chem. Soc*. **1956**, 4886.
(26) Rowe, I.; Post, B. *Acta Crystallogr*. **1958**, *11*, 372.
(27) Larson, S.; Simonsen, O.; Martin, G. E.; Smith, K.; Puig-Torres, S. *Acta Crystallogr.* **1984**, *C40*, 103.
(28) Gogonea, V.; Schleyer, P. v. R.; Schreiner, P. R. *Angew. Chem., Int. Ed. Engl.* **1998**, *37*, 1945. As described in this article, the magnetic shieldings for open-shell species are “unphysical”, but they are useful in examining the difference between local aromaticities of competing spin states.
(29) Klar, G.; Hinrichs, W.; Riedel, J. *J. Chem. Res*. **1982**, 334.
(30) Hinrichs, W.; Berges, P.; Klar, G. *Z. Naturforch. B* **1987**, *42*, 169.
(31) Matsuoka, M. Iwamoto, A.; Ouchi, T.; Yoshioka, H.; Nakatsu, K. *J. Heterocycl. Chem*. **1993**, *30*, 173.